Horizontal structure of unstable basin modes due to large scale baroclinic instability

Thierry Huck, Florent Aguesse, Patrice Bellec, Alain Colin de Verdière, Antoine Hochet, Quentin Jamet, Florian Sévellec, Jérôme Sirven

LPO>LOPS (UMR 6523 CNRS IFREMER IRD UBO), Brest, France

Drakkar Workshop, 28 January 2016, Grenoble

Abstract

Revisiting the classical wind-driven double-gyre in a 2.5 layer shallow water model, we show a regime of weak forcing/moderate viscosity (Reynolds number around 1) leading to decadal-scale oscillations. The unstable mode consists in baroclinically unstable Rossby waves in the northern part of the subpolar gyre. Their wavelength is set by the explicit model viscosity. Linear stability analysis alllows a proper energy budget of the modes highlighting the regions where the perturbations draw energy out of the mean flow. We discuss the limits of the 2.5 layer model where a single unstable vertical mode can exist, prohibiting the coexistence of large-scale Rossby waves (Green modes) and mesoscale variability (Charney modes). Unfortunately we have no example of such variability in oceanic observations...

Motivation

- context of Chaocean project (PI T. Penduff) rather than NEMO/Drakkar: sources of interannual ocean variability
- unstable basin modes with decadal period in PE models simplified configurations/forcing: constant buoyancy flux (Huck&al. 1999 JPO, Colin de Verdière&Huck 1999 JPO, te Raa&Dijkstra 2002 JPO...); but not unstable in 2-layer shallow-water models (Ferjani&al. 2013, 2014 JMR)
- large-scale baroclinic instability source of low-frequency oceanic variability (Hochet&al. 2015 JPO)
- Jamet&al. (2015 CD) with MIT GCM coupled model: difficult agreement between nonlinear oscillations T variance budget, "turbulent fluxes" and local instability

⇒ **simplest framework with large-scale baroclinic instability: 2.5-layer shallow water model** to allow clean analysis of local and global instability, and comparison with nonlinear oscillation and turbulent PV fluxes

Variability of the wind-driven circulation in idealized models

interannual variability arises when Reynolds number increases
$\mathrm{Re} = UL/\nu$
dynamical system approach > bifurcation structure in QG ou SW models: sensitivity to details like (free/no slip) boundary conditions, forcing symmetry... $\Rightarrow$ **gyre mode** (Nauw&Dijkstra 2001 JMR, Simonnet&Dijkstra 2002 JPO...)

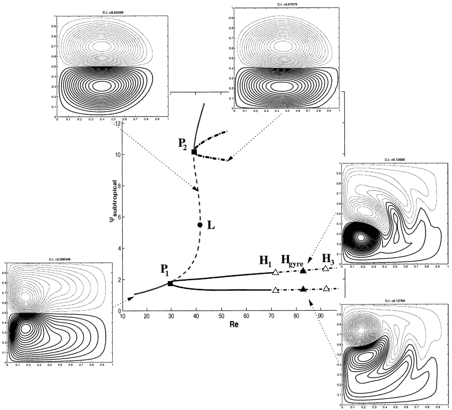

turbulent oscillator: positive feedback due to eddy rectification (Berloff&al. 2007 JPO)

2.5-Layer Shallow-Water Model Equations

$$\partial_t h_i + \nabla \cdot (h_i \, \mathbf{u_i}) = 0$$

$$\partial_t \mathbf{u_i} + \mathbf{u_i} \cdot \nabla \mathbf{u_i} + f \mathbf{k} \times \mathbf{u_i} = -\nabla \phi_i + \nu \nabla^2 \mathbf{u_i} + \delta_{i1} \frac{\tau}{\rho_i h_i}$$

$$\phi_1 = g'_{13} h_1 + g'_{23} h_2 \; ; \; \phi_2 = g'_{23} h_1 + g'_{23} h_2$$

$$g'_{ij} = g \frac{\rho_j - \rho_i}{\rho_j} > 0$$

h_i layer thickness, ϕ_i hydrostatic pressure/ρ_0
reduced gravity g'_{ij}: assumes 3^{rd} layer has infinite depth, null circulation/pressure gradient
forcing: zonal wind stress τ fct(latitude), constant in time
numerical resolution in Cartesian or spherical geometry: Arakawa C-grid with energy conserving scheme (Sadourny 1975) aka "ENE"
1/3° (1/6°)horizontal resolution $\Rightarrow$ Laplacian viscosity ν 3200 (400) m^2 s^{-1}

Configuration and forcing

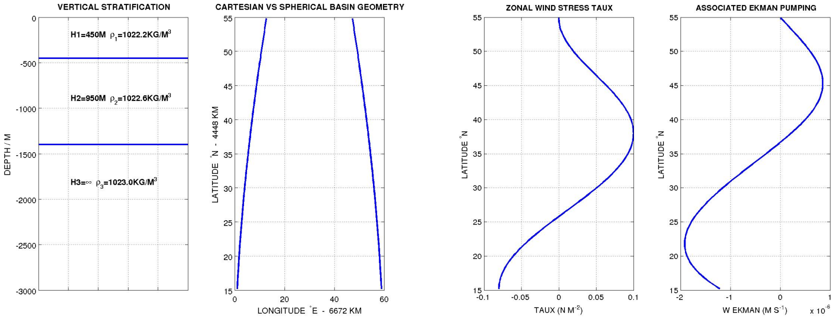

Vertical stratification, basin geometry and analytical wind forcing (zonal stress and Ekman pumping), identical to Sirven&al. 2015 JMR.

Control parameter: wind forcing amplitude, limited by upper layer outcropping for future linearization.

A flavor of the variability: oscillations with period O(7–8 yr)

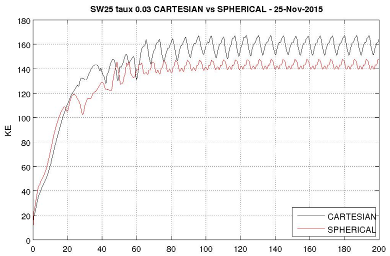

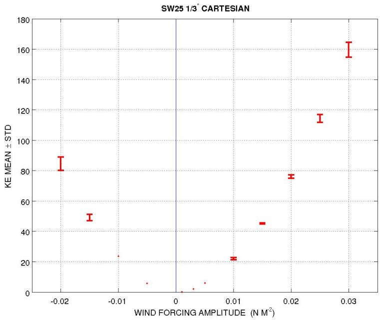

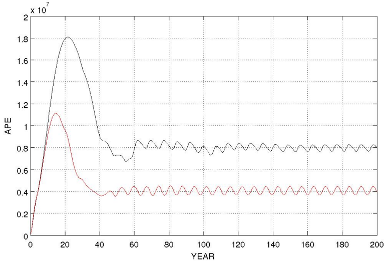

(left) Evolution of Kinetic Energy and Available Potential Energy for spherical and cartesian geometry.
(right) KE mean and standard deviation function of wind forcing (Cartesian geometry).
oscillation period set by stratification

Influence of increasing wind forcing amplitude

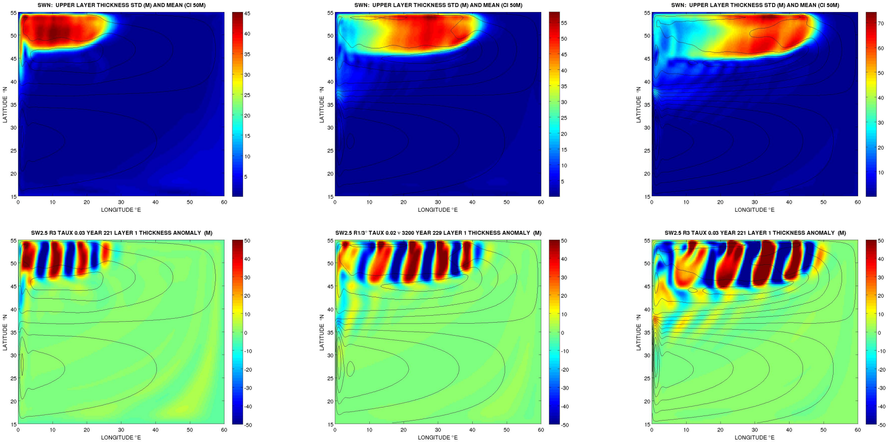

(top) Standard deviation and (bottom) anomaly of h_1 (color), superposed on the mean state (contours).

Variability increases and extends further east with increasing wind forcing: link with unstable regions?

Animation of h1' anomalies: westward propagation

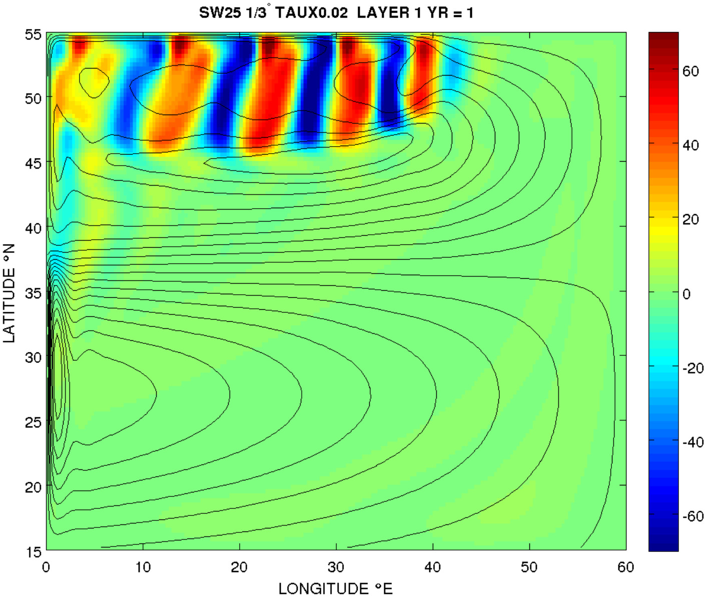

Regions of unstable waves propagation

$$\mathrm{PV}_i \approx \frac{f}{h_i}$$

North/45°N:

$\partial_y h_1 > 0 \Rightarrow$
$\partial_y \mathrm{PV}_1 < 0$

$\partial_y h_2 > 0 \Rightarrow$
$\partial_y \mathrm{PV}_2 > 0$

conditions for

baroclinic instability

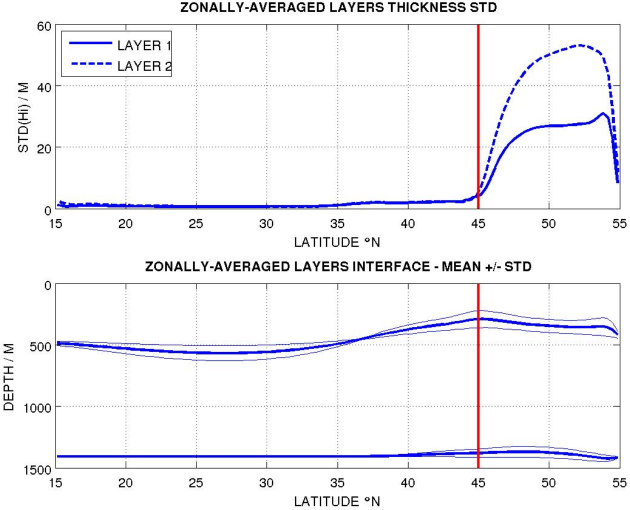

Conditions for baroclinic instability in SW2.5

Linear stability analysis of the 2.5 layer QG equations (Liu 1999 QJRMS)

- zonal mean flow U1 U2
- long wave approximation

⇒ analytical solutions

conditions for instability

U1<0 !

Hochet&al. 2015 JPO →

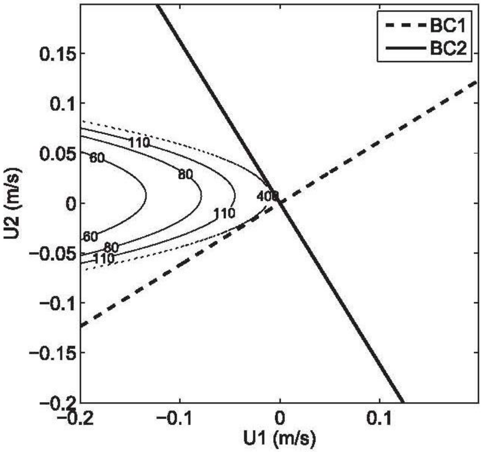

FIG. 1. Growth time (days) of large-scale modes in a 2.5-layer quasigeostrophic model as a function of the zonal velocities in layer 1 (U_1) and layer 2 (U_2). The zonal wavelength is 1000 km, and the latitude is 30°N. The two lines are the first (dashed) and second (solid) baroclinic modes; $H = 200$ m.

Relation with local baroclinic instability growthrate

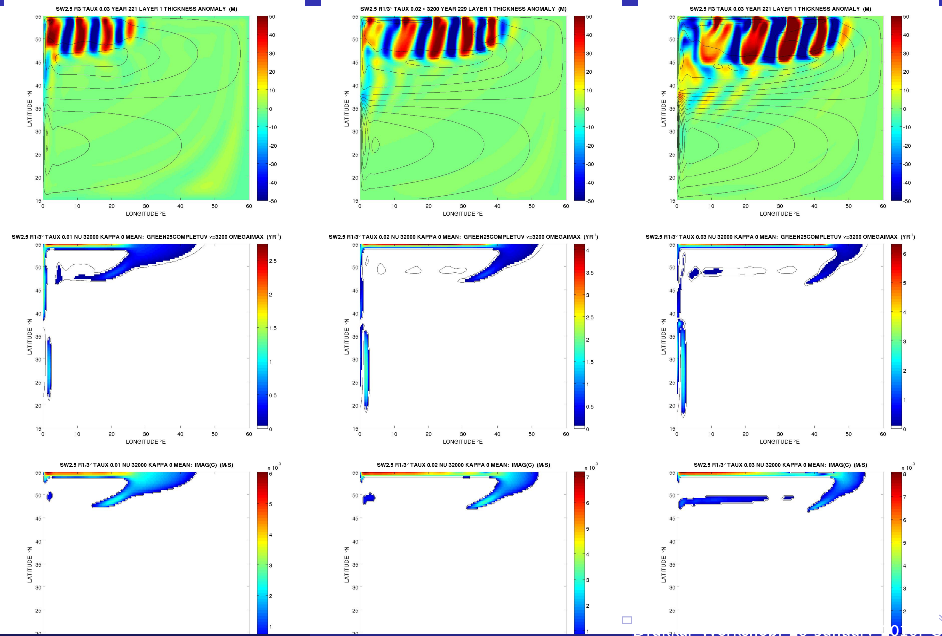

Selection of most unstable wavelength... by eddy viscosity

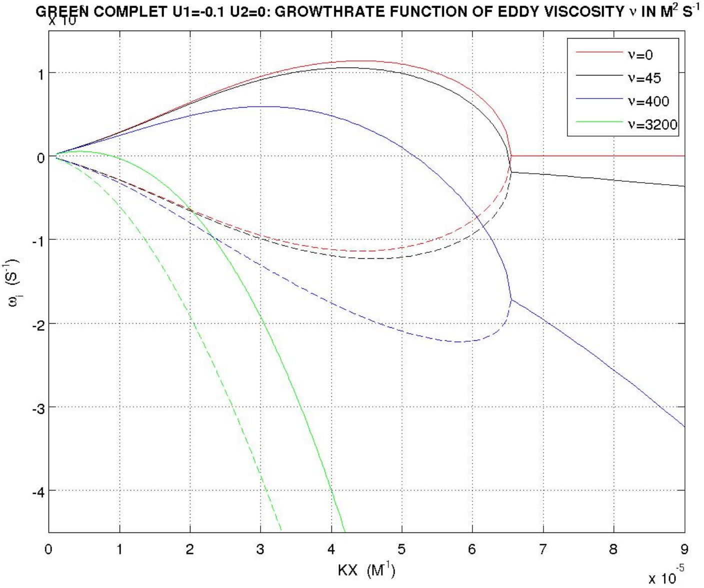

Closed PV contours in layer 2 define instability region

Rhines&Schopp 1991 JPO

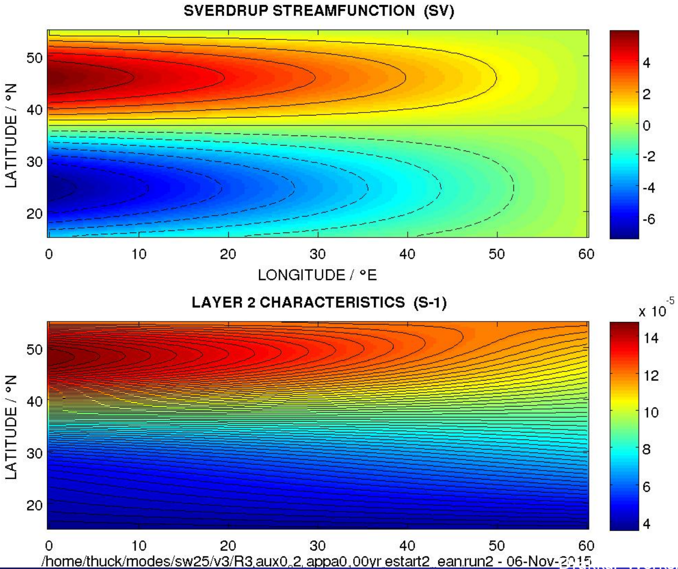

Reversed double gyre: instability at intergyre

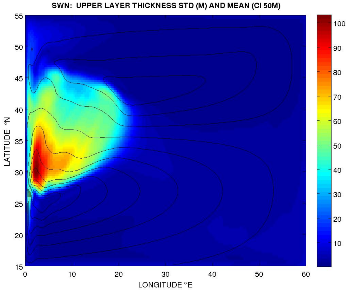

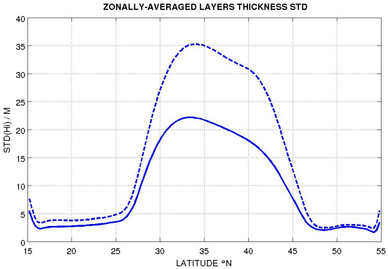

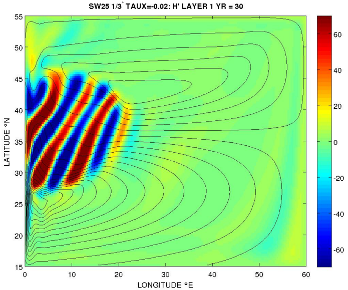

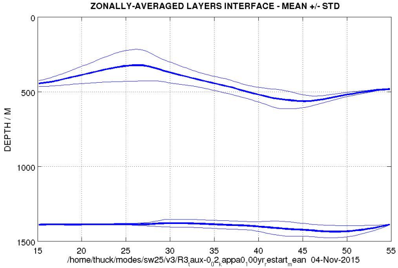

Reversed double gyre: Animation of h1'

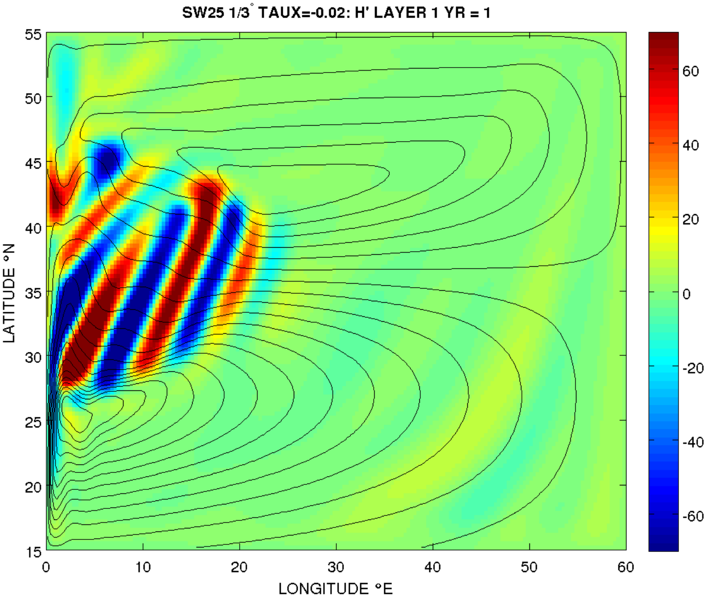

Classical double gyre with no momentum advection "PG"

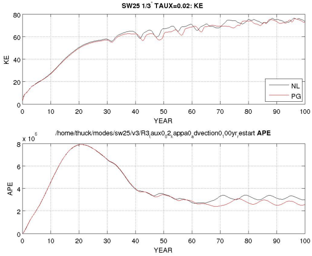

at 1/3°, planetary geostrophic dynamics makes almost no difference with full nonlinear equations

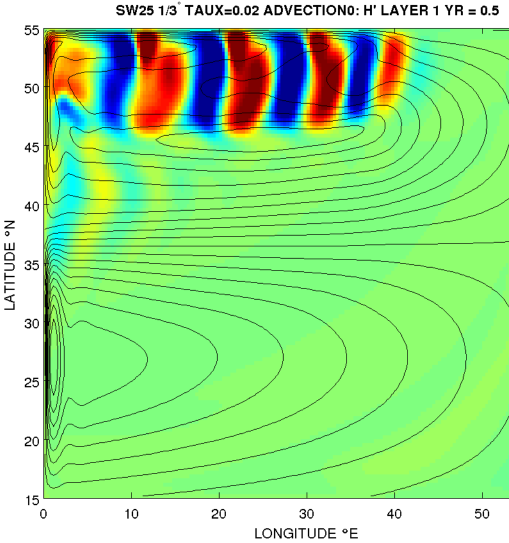

3D linear stability analysis > technical part

• linearized version of 2.5-layer SW model (no outcropping):
$X = \overline{X} + X'$, where $\overline{X}$ is steady or time-mean state

$$\partial_t h'_i + \nabla \cdot (\overline{h_i}\, \mathbf{u}'_\mathbf{i}) + \nabla \cdot (h'_i\, \overline{\mathbf{u}_\mathbf{i}}) = 0$$

$$\partial_t \mathbf{u}'_\mathbf{i} + \mathbf{u}'_\mathbf{i} \cdot \nabla \overline{\mathbf{u}_\mathbf{i}} + \overline{\mathbf{u}_\mathbf{i}} \cdot \nabla \mathbf{u}'_\mathbf{i} + f\mathbf{k} \times \mathbf{u}'_\mathbf{i} = -\nabla \phi'_i + \nu \nabla^2 \mathbf{u}'_\mathbf{i}$$

$$\phi'_1 = g'_{13} h'_1 + g'_{23} h'_2 \;;\; \phi'_2 = g'_{23} h'_1 + g'_{23} h'_2$$

• computation of eigenvalues of Jacobian J through those of propagator $M(\tau)$ with ARPACK: $\partial_t X = J\,X = \omega X$

$$X(t=0) \rightarrow X(t=\tau) = M(\tau)\,X(t=0) = e^{J\tau}\,X(t=0),$$

- initial perturbations $X(t=0)$ provided by iterative Arnoldi method,
- tangent linear model integrated for 'short' time, typically τ=0.1–0.3 yr,
- Jacobian eigenvalues ω deduced from propagator eigenvalues $e^{\omega\tau}$.

3D linear stability analysis: results

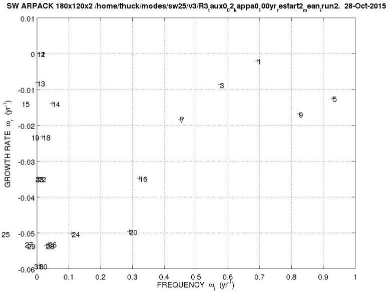

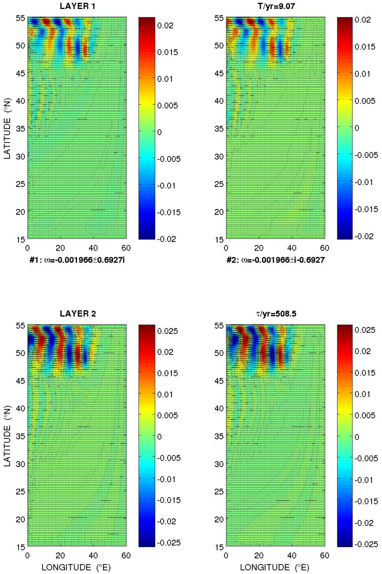

- leading eigenmode period 9 yr and wavenumber 4 similar to nonlinear oscillation
- all modes are stable on time-mean state: rectified by perturbations to remain marginally stable? (atmosphere)

Energy budget

- linear framework clearly separates perturbations from mean flow
- allows precise estimation of energy source and sink for modes
- sucessfully used in barotropic shallow water model (Herbette&al. 2014 GAFD) to determine regions of barotropic instability sustaining oscillation
- extended here to address baroclinic modes where APE » KE

Energy budget equations

Multiplying momentum equations by $(h_i \mathbf{u_i})$:

$$\partial_t \left[h_i \frac{|\mathbf{u_i}|^2}{2} \right] + \nabla \cdot \left[h_i \mathbf{u_i} \frac{|\mathbf{u_i}|^2}{2} \right] = -h_i \mathbf{u_i} \cdot \nabla \phi_i = -\nabla (h_i \mathbf{u_i} \phi_i) - \phi_i \, \partial_t h_i$$

Summing last rhs term for the 2 layers leads to natural definition of APE:

$$\begin{aligned} \sum_i \phi_i \, \partial_t h_i &= (g'_{13} h_1 + g'_{23} h_2) \, \partial_t h_1 + (g'_{23} h_1 + g'_{23} h_2) \, \partial_t h_2 \\ &= \partial_t \left(g'_1 \frac{h_1^2}{2} + g'_2 \frac{h_2^2}{2} + g'_2 h_1 h_2 \right) \end{aligned}$$

In terms of interface deviations η_i

$$\mathrm{APE} = g \frac{\eta_1^2}{2} + g'_{12} \frac{\eta_2^2}{2} + g'_{23} \frac{\eta_3^2}{2}$$

Energy budget for leading mode... (work in progress)

points to large source region along northern boundary

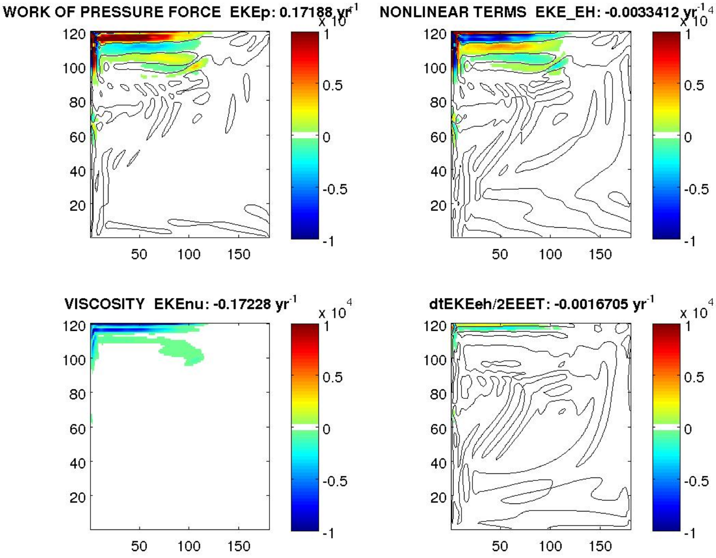

Influence of resolution and dissipation: 1/6°, ν=400 m^2 s^{-1}

shorter wavelength and more irregular oscillations

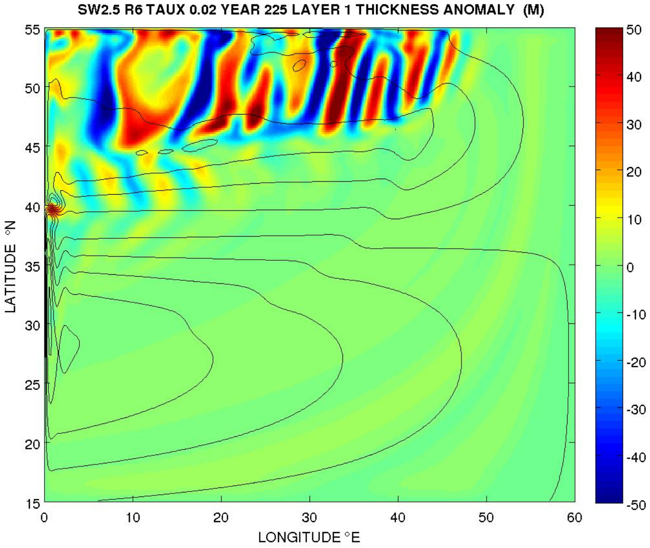

The limits of crude vertical resolution

single vertical structure of unstable mode mix longwave Green type and mesoscale Charney type instability (Beckmann 1988 JPO)

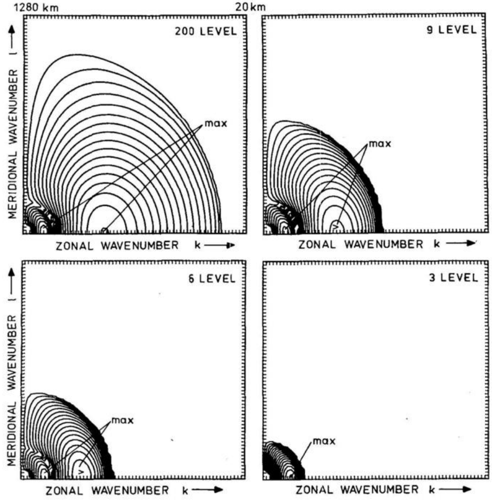

FIG. 5. Spectral distribution of maximum growth rate of unstable shear modes depending on the vertical resolution of the model. The maximum lies on the *k*-axis. Contour interval: 10^{-7} s^{-1}.

[Beckmann 1988 JPO]

Discussion & Conclusions

Peculiar regime of wind-forced ocean circulation:
weak forcing (1/3) and moderate dissipation ⇒ Reynolds number O(1), not described in the litterature as far as I know?
Problem: unstable modes wavelength set by dissipation! most likely due to too crude vertical resolution.

Stronger forcing? leads to upper layer outcropping, variability regions shift to intergyre outcropping, waves become more nonlinear
Signature of these modes in oceanic variability? to be compared to response to varying wind forcing (Sirven&al. 2015 JMR)

first methodological step related to Quentin Jamet PhD thesis (2015) trying to reconcile various analysis of variability in simplest framework: density variance budget and eddy fluxes $\overline{u'h'}\nabla\overline{h}$, vs. local and global linear stability analysis

▷ similar ocean observations? maybe in the tropics...

THANK YOU FOR YOUR ATTENTION